Steam Reforming of Bio-Compounds with Auto-Reduced Nickel Catalyst

Feng Cheng and Valerie Dupont *

School of Chemical and Process Engineering, University of Leeds, Leeds LS2 9JT, UK; fengcheng@njust.edu.cn
* Correspondence: V.Dupont@leeds.ac.uk; Tel.: +44-113-343-2503

Abstract: As an extension of chemical looping combustion, chemical looping steam reforming (CLSR) has been developed for H_2 production. During CLSR, a steam reforming (SR) process occurs following the reduction of catalysts by the reforming feedstock itself (termed "auto-reduction"), as opposed to a separate, dedicated reducing agent like H_2. This paper studied SR performances of four common bio-compounds (ethanol, acetone, furfural, and glucose) with a nickel catalyst that had undergone auto-reduction. A packed bed reactor was used to carry out the experiment of auto-reduction and subsequent SR. The effects of temperature and steam to carbon ratio (S/C) on the carbon conversions of the bio-compounds to gases and yields of gaseous products were investigated. The carbon deposition on spent catalysts was characterized by CHN elemental analysis and Scanning Electron Microscopy-Energy Dispersive X-ray Spectroscopy (SEM-EDX). The SR performance with the auto-reduced catalyst was close to that with the H_2-reduced catalyst. In general, an increase in temperature or S/C would lead to an increase in H_2 yields. The dependence of SR performance on temperature or S/C was specific to the type of bio-compounds. Accordingly, the main bottlenecks for SR of each bio-compound were summarized. A large amount of CH_4 existed in the reforming product of ethanol. Severe carbon deposition was observed for SR of acetone at temperatures below 650 °C. A high thermal stability of furfural molecules or its derivatives restricted the SR of furfural. For SR of glucose, the main problem was the severe agglomeration of catalyst particles due to glucose coking.

Keywords: nickel catalyst; steam reforming; model compound; bio-oil; auto-reduction

1. Introduction

Nowadays, H_2 is mainly produced from fossil fuels through thermochemical processes such as catalytic steam reforming, partial oxidation, and gasification, followed by a water gas shift (WGS) reaction. Sustainable H_2 production from renewable energy sources is crucial to the realization of the 'hydrogen economy' and meeting the increasing demands in synthetic fertiliser as well as hydrotreating processes in refineries and biorefineries in the future. Biomass is an important renewable energy source due to its characteristics of continuous supply via photosynthesis, CO_2 neutrality, and low sulphur content. Steam reforming (SR) of bio-oil, a liquid product of biomass fast pyrolysis, is one of the promising ways to produce H_2 from biomass [1]. Aqueous phase reforming is another technology for H_2 production from biomass-derived compounds [2]. Glucose and biomass-derived polyols (ethylene glycol, glycerol, sorbitol, etc.) have been successfully applied in this process. However, bio-oil is not suitable for aqueous phase reforming as bio-oil cannot completely dissolve in water.

Bio-oil is a complex mixture consisting of various oxygenated hydrocarbons. By adding water, bio-oil can be separated into two immiscible phases: an aqueous phase and a hydrophobic phase. According to molecular structures, the components of bio-oil generally fall into seven chemical

families: carboxylic acids, aldehydes, alcohols, ketones, sugars, furans, and phenols [3]. The complex composition of bio-oil leads to a complicated reaction network and coking mechanism during SR of bio-oil. In order to better understand this process, SR of single bio-oil components (termed "bio-compound") was investigated by experiments [4–10] or simulation calculations [11–14]. Bio-compounds that have been subjected to SR studies include ethanol [15–19], acetic acid [7,13,20], ethylene glycol [13], glycerol [21], hydroxyacetaldehyde [7], acetone [10], acetol [9], ethyl acetate [10], glucose [5,10], xylose [5], sucrose [5], *m*-cresol [5,22], *m*-xylene [10], di-benzyl ether [5], methanol [23], phenol [24], etc.

The SR performance (normally indicated by carbon conversion of feedstock to gases, H_2 yield, and carbon deposition) varies with the catalyst and the condition applied. Therefore, it is not easy to find consistency between the results from different research groups despite the use of the same bio-compound. High H_2 yields and thus the feasibility of these bio-compounds for SR were usually reported, but less attention has been paid to process characteristics that are specific to individual bio-oil components. Hu and Lu [25] investigated the effects of molecular structure on the SR performance of bio-oil components. The type of functional group significantly affected steam reforming. Alcohol steam reforming tended to produce a significant amount of CH_4, which was influenced by the length of the carbon chains, and the number and the location of hydroxyl groups. Severe coke deposition was encountered in the steam reforming of ketone compounds such as acetone. Hu and Lu [10] also compared the coking rate of different bio-oil components during a SR process and discussed the coking mechanism of different bio-oil components. They reported that decomposition or polymerization of the feedstocks were main routes for coke formation in glucose, m-xylene, and acetone reforming. The large amounts of by-products such as ethylene, CO, or acetone were coke precursor in the SR of acetic acid, ethyl acetate, and ethylene glycol. Remon et al. [26] studied the influence of bio-oil composition on the SR result. A strategy was established to identify the chemical compounds that were responsible for the most significant variations observed during SR of the bio-oil. The SR results were greatly affected by the proportion of acetic acid and furfural in the bio-oil. Compared to acetic acid, furfural had a high tendency to produce coke in a reforming process.

Chemical looping steam reforming (CLSR, also termed unmixed steam reforming) is an advanced steam reforming technology [27–31]. It has a similar basic principle as chemical looping combustion (CLC), whereas the main difference is that the target product of CLSR is syngas rather than heat in CLC [32]. High-purity H_2 could be obtained if passing the syngas from CLSR through a water gas shift (WGS) reactor. During a CLSR process, either a supported metal oxide circulates between an air reactor and a fuel reactor (recirculating fluidised bed configuration), or an air/fuel feed flows alternately over a packed bed reactor, in which case at least two reactors are needed for the production of a continuous H_2 output. In a fuel reactor or under a fuel feed flow, the metal oxide is reduced by the fuel first and then catalyses the subsequent SR reaction of the fuel. In the air reactor or under an air flow, the reduced metal oxide is oxidized by air. Obviously, the supported metal oxide performs both the roles of oxygen carrier and SR catalyst. The reduction of the metal oxide by fuel is a necessary and key step for a CLSR process. If H_2 is used to reduce the catalyst instead of fuel during a CLSR process, the operation complexity will increase although better reduction kinetics and free carbon deposition can be achieved. Compared with conventional SR, CLSR has several advantages [31,33]: (a) A more uniform supply of heat to the endothermic SR reaction can be achieved by the internal unmixed combustion. (b) The coked catalyst can be cyclically regenerated by combusting the coke in the air reactor. (c) No external heat is needed if the process is designed properly (i.e., autothermal CLSR). (d) The CLSR configuration is easy to integrate with in situ CO_2 adsorption by adding sorbents such as CaO in the bed materials. The CLSR system integrated with in situ CO_2 adsorption is termed "sorption enhanced chemical looping steam reforming" (SE-CLSR), a process that can generate H_2 with >90% purity [34,35]. Extensive studies have been devoted to CLSR of natural gas. It is generally believed that supported NiO is a promising oxygen carrier for CH_4 CLSR due to its high reduction reactivity and good catalytic activity for SR once NiO is reduced to Ni [32,36]. Actually, alumina supported NiO

(NiO/α-Al$_2$O$_3$) is a common reforming catalyst in industry [37]. Similar to other transition metal catalysts, NiO catalysts require reduction to yield the active phase (i.e., metallic Ni) prior to their use in a SR process. The catalyst reduction is usually conducted with either hydrogen-containing gases or natural gas-steam mixtures [38]. Catalytic activity, sulphur poisoning, carbon deposition, and nickel sintering are four challenges faced by nickel reforming catalysts [39].

Recently, some renewable liquid feedstock such as bio-oil [40], glycerol from bio-diesel production [34], vegetable oil [41], waste cooking oil [28,35], pyrolysis oil of scrap tyre [29], and tar from biomass gasification [32] have been tested in a CLSR process using NiO catalysts. Considering the complexity of these bio- and waste-derived liquids, it is necessary to study the CLSR performance of typical bio-compounds. The CLSR performance needs to be evaluated from three aspects: (1) direct reduction of the catalyst by the bio-compound (termed "auto-reduction" to differentiate the reduction with H$_2$), (2) SR of the bio-compound with the auto-reduced catalyst, and (3) cyclic performance of the two processes above. The authors have investigated the auto-reduction of a NiO/α-Al$_2$O$_3$ catalyst with acetic acid and subsequent SR of acetic acid [42]. Results showed that a steady SR regime along with complete NiO reduction could be achieved after a coexistence stage of reduction and reforming. The SR activity of the auto-reduced catalyst was just below that of the H$_2$-reduced catalyst, probably attributed to the formation of denser carbon filaments and associated larger loss of active Ni. Apart from acetic acid, a series of other bio-compounds (ethanol, acetone, furfural, glucose) have also been examined for the reduction of a NiO/α-Al$_2$O$_3$ catalyst [36]. The feasibility of catalyst auto-reduction was proven. The effects of temperature and steam content on reduction kinetics were systematically analysed.

However, the SR performance of these bio-compounds with the auto-reduced nickel catalyst has not been reported yet, which is the concern of this paper. First, the SR activity of the auto-reduced catalyst was compared to that of the H$_2$-reduced catalyst. Second, the effects of temperature and steam to carbon ratio (S/C) on the SR performance were investigated for each bio-compound. As a special case of S/C dependency, the catalytic pyrolysis of bio-compounds (i.e., S/C = 0) was also studied. Finally, the main barriers for each bio-compound in a SR process were summarised. In order to make an overall comparison among different bio-compounds, the data of acetic acid SR published in [42] was cited in this paper. The work presented here is part of the PhD thesis of the first author [43]. The objective of this paper is to identify the process characteristics of each bio-compound in the SR process and show the dependence of these characteristics on temperature or S/C. The influence of reaction time on the SR performance was not considered in this work. A complete CLSR process that integrates catalyst oxidation, catalyst auto-reduction, and SR of fuels will be investigated in the next work.

2. Results and Discussion

2.1. Comparison between Auto-Reduction and H$_2$ Reduction

SR performances of ethanol, acetone, and furfural with the auto-reduced nickel catalyst are presented in Figure 1 (solid line). A CO$_2$ emission peak and a H$_2$O generation peak that appeared at the initial stage indicated the occurrence of auto-reduction [42]. Following the auto-reduction, a stable SR performance (represented by feedstock conversions and H$_2$ yields) was shown over the duration of 45–60 min. The SR performance with the auto-reduced catalyst was quite close to that with the H$_2$-reduced catalyst (dotted line in Figure 1). This result suggested that using ethanol, acetone, or furfural instead of H$_2$ to activate the catalyst had a negligible influence on its catalytic activity. In contrast, the catalyst auto-reduced by acetic acid showed a slightly lower catalytic activity than the H$_2$-reduced catalyst [42]. The decrease in the catalytic activity was tentatively ascribed to the loss of active metal Ni during the catalyst auto-reduction with acetic acid. Fluctuations of feedstock conversion and gas product yields were observed for the SR of furfural (Figure 1c-1,c-2) and later for the catalytic pyrolysis of furfural (Figure 8d). The low volatility of furfural might be responsible for these fluctuations. Due to the low volatility, the droplets of

furfural might fall on the catalyst bed directly before they were completely vaporized. As a result, the gas stream was disturbed and went through the gas analyser like pulses.
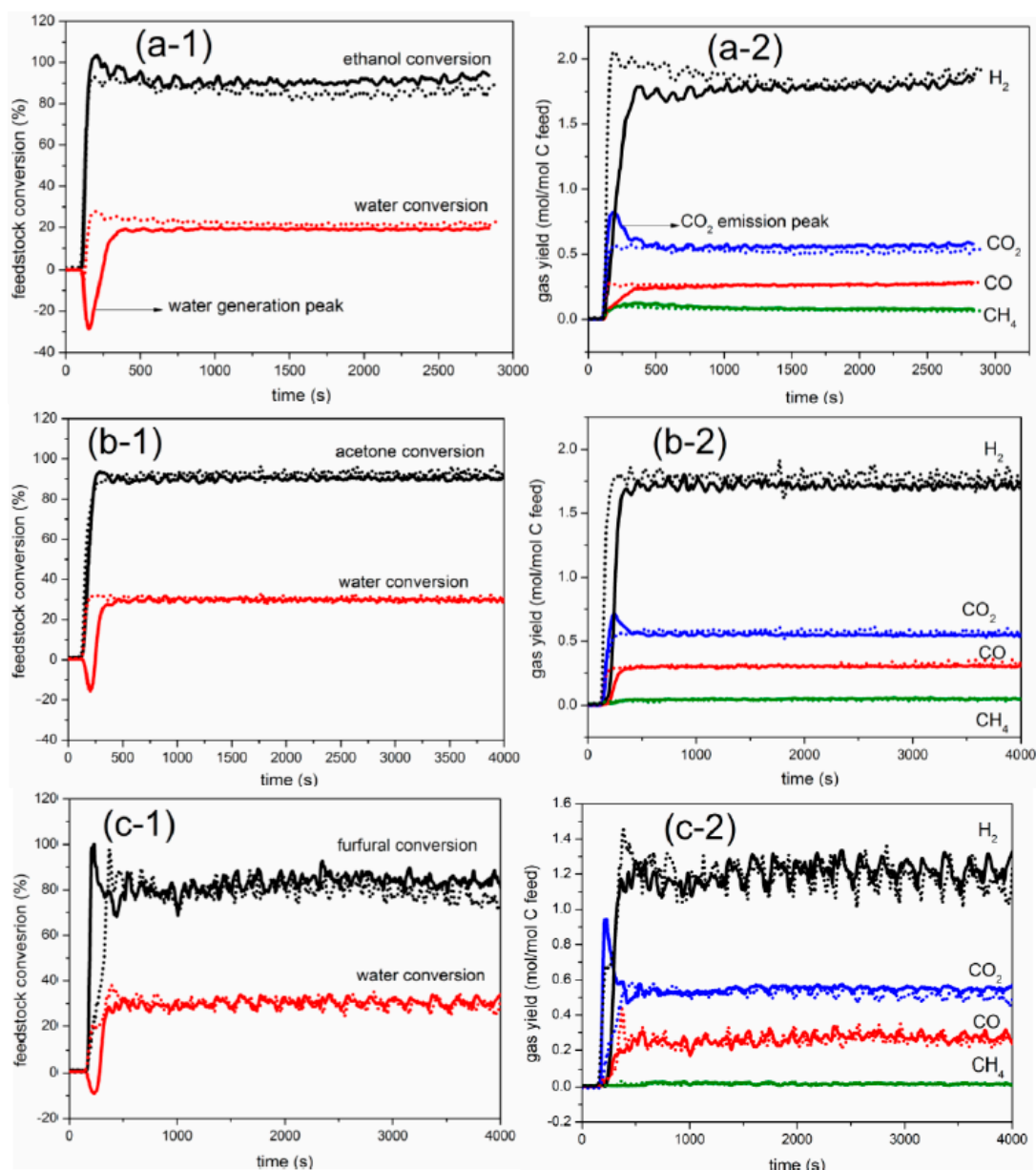

Figure 1. Steam reforming (SR) performance comparison between auto-reduction (solid line) and H_2 reduction (dotted line) at 650 °C, steam to carbon ratio S/C = 3: (**a-1**) conversions of ethanol and water, (**a-2**) gas product yields during SR of ethanol; (**b-1**) conversions of acetone and water, (**b-2**) gas product yields during SR of acetone; (**c-1**) conversions of furfural and water, (**c-2**) gas product yields during SR of furfural.

2.2. Effects of Temperature

2.2.1. Carbon Conversion of Bio-Compounds to Gases

Figure 2 shows the dependence of the carbon conversions of the bio-compounds on temperature during SR with the auto-reduced nickel catalyst. According to the variation trend, the five bio-compounds could be categorized into two groups. For the light bio-compounds (acetic acid, ethanol, and acetone), their conversions increased progressively as the temperature rose. As for the bio-compounds with larger molecular structures (i.e., furfural and glucose), their conversions hardly varied with temperature until the temperature was raised to 600 °C. Above 600 °C, their

conversions exhibited an increasing trend with temperature, similar to that observed for the light bio-compounds. Therefore, the bottleneck temperature for an effective conversion of glucose or furfural to gaseous products was 600 °C. An operation temperature for SR of furfural or glucose was suggested to be 650 °C or above. At 650 °C, the bio-compound conversion decreased in this order: ethanol ≈ acetone > glucose > furfural > acetic acid. It was noticed that the conversion of ethanol was incomplete even at 750 °C, indicating that the catalyst used, a commercial catalyst for CH_4 SR, may be not very suitable for the SR of oxygenated hydrocarbons.
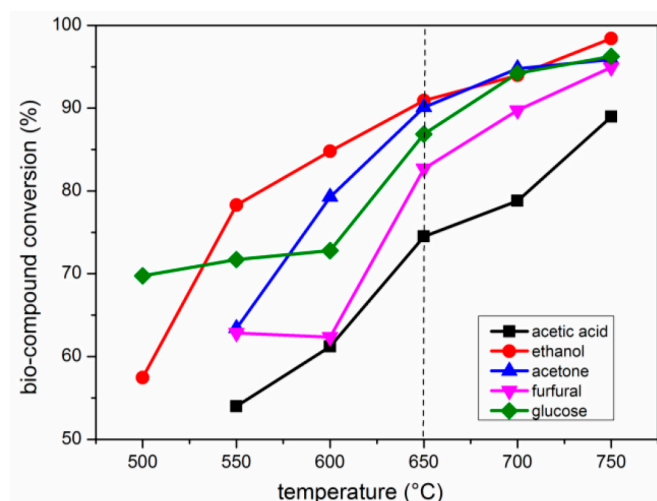

Figure 2. Effects of temperature on bio-compound conversion during SR with the auto-reduced catalyst (S/C = 6 for glucose, S/C = 3 for the rest).

The photos of condensate samples collected from the furfural experiments are shown in Figure 3. A considerable volume of condensate with yellow colour was produced at 550 and 600 °C, indicating that there were some unreacted furfural molecules or its derivatives (e.g., furan) in the condensate. Kato et al. [44] found that furfural was fairly thermally stable and about 90% remained unchanged when heating furfural at 500 °C. When increasing the SR temperature from 600 to 650 °C in this work, the amount of condensate dramatically decreased and the colour became transparent. This result was in good agreement with the remarkable increase of the furfural conversion from 600 to 650 °C (Figure 2). It is common that unreacted feedstock molecules or their liquid intermediates are found in the condensate when using heavy bio-oil compounds for SR [45]. This not only represents a waste of resources but also causes pollution if the condensate is not disposed of properly. Wu and Liu [45] proposed an operation of liquid condensate recycling for the SR of heavy bio-oil components. With this operation, the liquid pollutant was eliminated completely and the carbon deposition was reduced effectively.
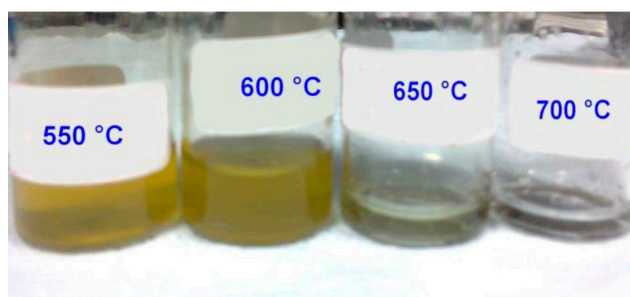

Figure 3. Photos of condensate samples collected from furfural SR experiments at different temperatures with S/C = 3.

The thermal stability of furfural molecules [44,46] limited SR of furfural at low temperatures, while the severe agglomeration of catalyst particles was the main problem for SR of glucose. As

Figure 4 shows, the agglomeration extent decreased as the temperature increased and was eliminated at 700 °C.
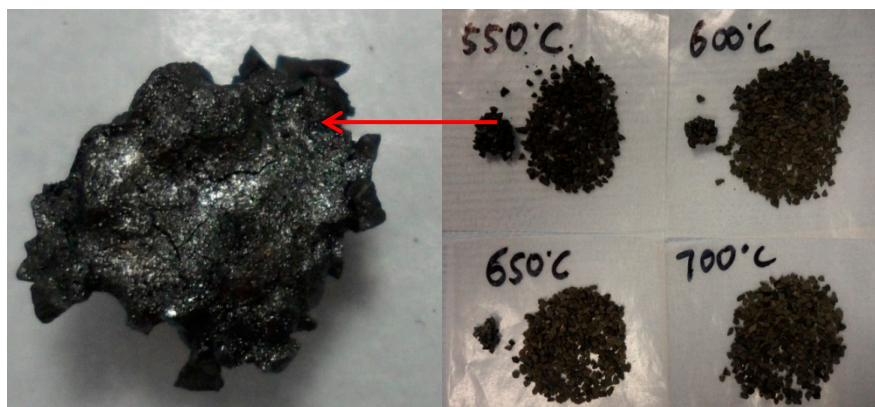

Figure 4. Photos of the spent catalysts collected from the glucose SR experiments at different temperatures with S/C = 6.

Figure 4 clearly shows that the agglomeration of catalyst particles was caused by the coking of glucose. Thermal degradation of glucose was a complex process, consisting of fragmentation, polymerization, isomerisation, and dehydration [46–48]. Various oligo- and poly-saccharides as well as the brown caramel matter formed in this process [48] might act as glue to combine the catalyst particles together. Possible reaction pathways of the 'sugar glue' at different temperatures are illustrated in Figure 5. At low temperatures (e.g., 550 °C), the 'sugar glue' decomposed slowly and formed coke. When the temperature was high (e.g., 700 °C), the 'sugar glue' decomposed rapidly and produced small molecules that could be easily reformed. Hence, the agglomeration of catalyst particles was eliminated. CHN elemental analysis suggested that the carbon content in the non-agglomerated catalyst particles was small (1.4 wt % at 550 °C and 0.5 wt % at 700 °C), lower than that reported in the literature [10]. In order to achieve an effective SR of glucose or bio-oil that contains glucose, the agglomeration of catalyst particles must be eliminated first by elevating operation temperatures or by other methods. In addition, the coking rate of this catalyst is still too high for a real application. Hence, further modifications of the catalyst are required.
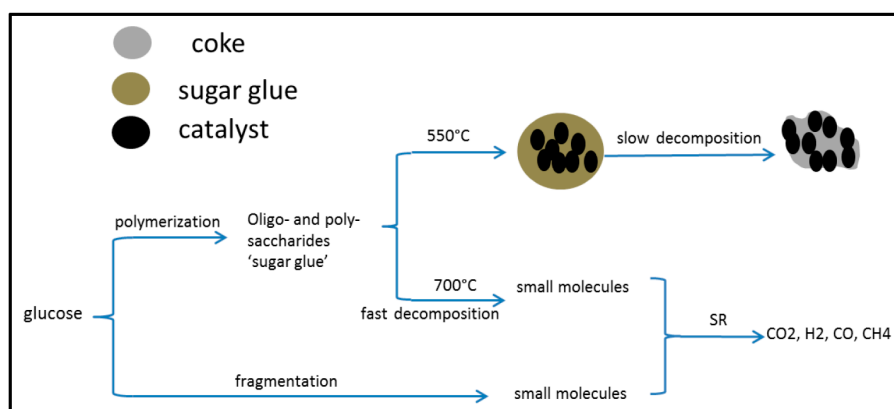

Figure 5. Schematic diagram for the possible reaction pathways during the SR of glucose.

2.2.2. Yield of Gaseous Products

Figure 6 presents the gas yields from SR of bio-compounds with the auto-reduced catalyst. As Figure 6a shows, the variation trend of the H_2 yield with temperature was similar to that of bio-compound conversion (Figure 2), indicating the dependence of the H_2 yield on bio-compound conversion. Generally, a higher bio-compound conversion means more H_2 being generated. In addition, the potential of a bio-compound for H_2 production (i.e., equilibrium H_2 yield) also plays a

role in determining the H_2 yield. For instance, the H_2 yield decreased in this order: ethanol > acetone > glucose, although the conversions of the three bio-compounds are approximated to each other above 650 °C (see Figure 2). This was because the equilibrium H_2 yield decreased in the order ethanol > acetone > glucose as Table 1 shows. Above 650 °C, the experimental H_2 yield decreased in the order of ethanol > acetone > glucose > furfural > acetic acid. The SR of ethanol achieved the largest H_2 yield (1.78 mol/mol C feed at 650 °C, 69% of the equilibrium potential) while the H_2 yield from SR of acetic acid was the lowest (1.06 mol/mol C feed at 650 °C, 61% of the equilibrium potential).
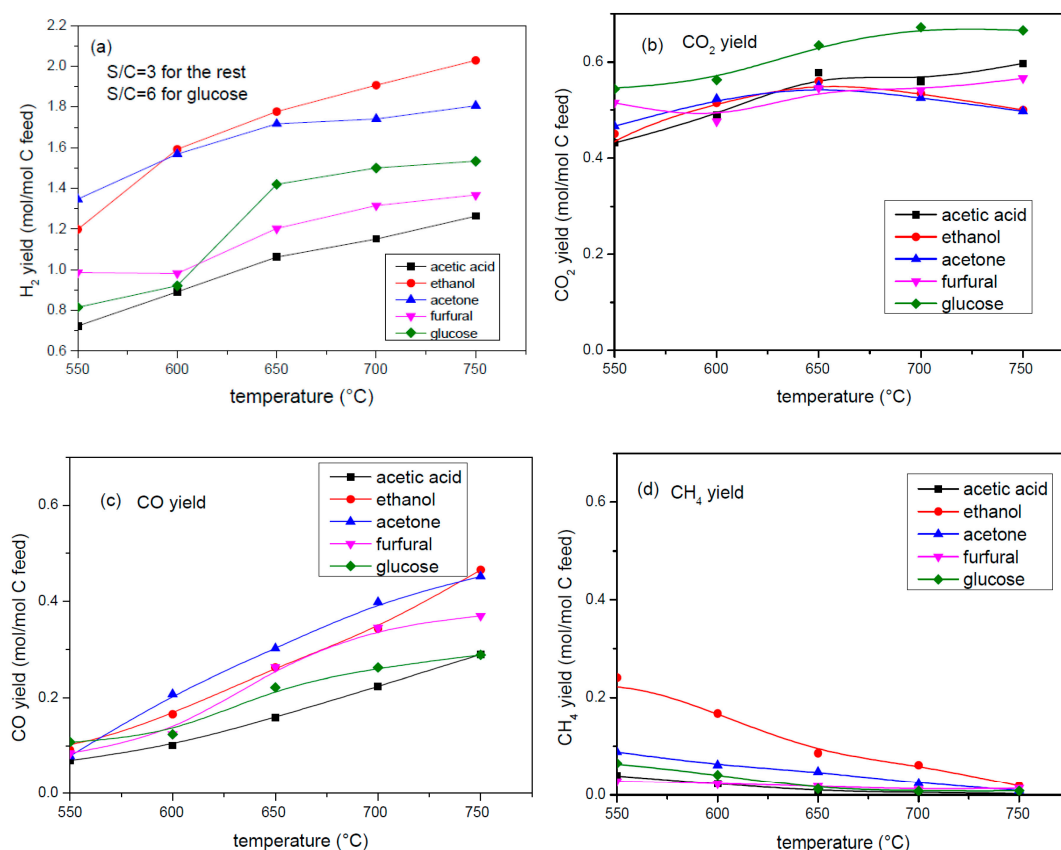

Figure 6. Influences of temperature on gas yields from steam reforming of bio-compounds with the auto-reduced nickel catalyst (S/C = 6 for glucose, S/C = 3 for the rest): (**a**) H_2, (**b**) CO_2, (**c**) CO, and (**d**) CH_4.

Table 1. H_2 yields (in mol/mol C feed) from SR of different bio-compounds at 650 °C, S/C = 6 for glucose and S/C = 3 for the rest.

Bio-Compound	Stoichiometric [1]	Equilibrium [2]	Experiment	H_2 Yield Efficiency (%)
ethanol	3	2.58	1.78	68.99
acetone	2.7	2.26	1.72	76.11
glucose	2	1.85	1.42	76.76
acetic acid	2	1.73	1.06	61.27
furfural	2	1.67	1.20	71.86

[1] according to the SR reaction equations with CO_2 and H_2 as the final products; [2] obtained by Chemical Equilibrium with Application (CEA) thermodynamic equilibrium calculation.

The influence of temperature on the CO_2 yield was not remarkable as Figure 6b shows. With the rising temperature, the total amount of gaseous products increased due to an increasing bio-compound conversion. Meanwhile, the CO_2 concentration in the products decreased (see Supplementary Materials Figure S1) because the WGS reaction, which contributed to the

production of CO_2, was unfavoured at elevated temperatures. The balance between these two factors resulted in a negligible variation of the CO_2 yield with temperature.

In contrast, the dependence of CO production on temperature was more pronounced (Figure 6c). The CO yield showed a linear growth with temperature. This growth could be attributed to two reasons: (1) the increasing bio-compound conversion which produced more CO, (2) the weakened WGS reaction which decreased the conversion of CO to CO_2.

A linear decreasing trend was found for the CH_4 yield as the temperature rose (Figure 6d), probably because the elevated temperatures promoted both the chemical equilibrium and reaction kinetics of CH_4 SR. At 750 °C, the CH_4 yield was almost zero for all the bio-compounds. Below 750 °C, the ranking of bio-compounds in terms of CH_4 yield was as follows: ethanol > acetone > (furfural = glucose = acetic acid). The largest CH_4 yield was obtained from SR of ethanol, which may relate to the fact that a large amount of CH_4 was produced via ethanol decomposition (see Table 2). Lu and Hu [10] also found that the CH_4 selectivity was higher in SR of the neutral fuels (ethanol, 1-propanol) than in SR of the acidic fuels (acetic acid, propanoic acid). They suggested that the acidification of neutral alcohols with nitric acid could suppress the CH_4 formation.

2.2.3. Yield of Carbon Deposits

During SR of bio-oil or bio-oil fraction, oxygenated hydrocarbons tend to decompose and form solid carbonaceous materials on the catalyst. The Boudouard reaction is another common reaction for carbon formation during SR. The Boudouard reaction ($2CO \leftrightarrow CO_2 + C$), which is exothermic, may be dominant for carbon formation at low temperatures while the carbon formation by thermal decomposition was more favoured at high temperatures. The carbon deposition is a main problem faced by SR of bio-oil as it not only impairs the catalyst activity but also causes some operational problems such as blocking the reactor, crushing the catalyst pellets. Hence, it is important to study the carbon deposition behaviour of the different bio-compounds. Figure 7 shows the yields of carbon deposits from SR of acetic acid, ethanol, acetone, and furfural at different temperatures.
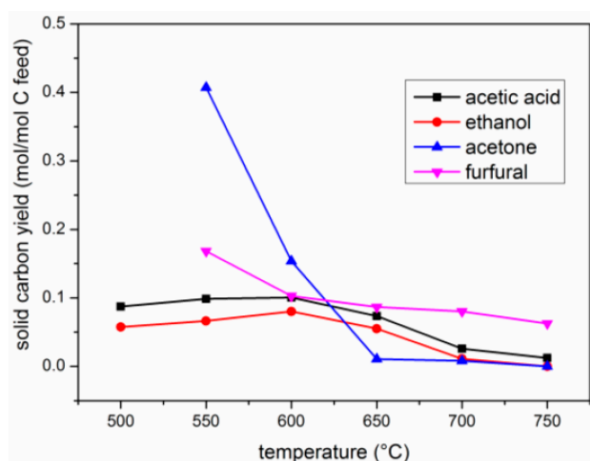

Figure 7. Yields of carbon deposits on the reacted catalyst at different temperatures with S/C = 3.

In the SR of acetic acid and ethanol, the yield of the carbon deposits slightly increased first and then decreased with the maximum yield appearing at 600 °C. Wu and Liu [22] proposed a carbon deposition-carbon elimination kinetic model to explain a peak value of carbon formation observed for SR of cresol. In a catalytic SR process, carbon deposition and carbon elimination coexist. Both the reaction rates increase with the temperature. The apparent carbon formation rate is determined by the competition of the two reactions. According to this kinetic model, it could be deduced that the carbon deposition (e.g., by thermal decomposition) was more favoured by the temperature rise from 500 to 600 °C than the carbon elimination (e.g., by steam gasification). The opposite was the case in a higher temperature region (600–700 °C). Above 700 °C, the influence of temperature on the carbon deposition was negligible and the solid carbon yields were low, only 2.59% and 1.11% of the

C input, respectively. For the SR of acetone, its solid carbon yield at 550 °C was extremely high, about 40%. As the temperature increased, the solid carbon yield from SR of acetone decreased sharply until 650 °C, above which the solid carbon yield was almost zero. Accordingly, the practical operation temperature for SR of bio-oil that contains a large amount of acetone is suggested to be above 650 °C so that carbon deposition could be mitigated. For the SR of furfural, its solid carbon yield also decreased first and then levelled off around 8% when the temperature was beyond 600 °C. This result suggests that raising the temperature is not an effective approach to reduce carbon deposits during SR of furfural; although it could enhance furfural conversion and H_2 yield (see Sections 2.2.1 and 2.2.2). To overcome the severe carbon deposition and thus avoid catalyst deactivation, the design and synthesis of an adequate catalyst is desirable.

Comparing the different bio-compounds, the correlation between carbon deposition and SR performance (conversion of feedstock, H_2 yield) was not clear. For example, the H_2 yield at 650 °C and S/C = 3 decreased in this order: ethanol > acetone > furfural > acetic acid, whereas the amount of carbon deposits increased in the order: acetone < ethanol < acetic acid < furfural. This is because the SR performance is determined by several factors including the intrinsic property of bio-compounds and the catalyst activity. The catalyst activity is mainly affected by carbon deposition if the same catalyst material and the same reaction conditions are applied. Different bio-compounds may have different tendencies to form carbon deposits [10,25,26]. In this paper, the SR performance heavily depended on the intrinsic property of feedstock and poorly correlated with the carbon deposition.

2.3. Catalytic Pyrolysis of Bio-Compounds (S/C = 0)

Before studying the effect of S/C on SR performance, the special case S/C = 0 was investigated at 650 °C and in the presence of the NiO/α-Al$_2$O$_3$ catalyst. Figure 8 displays the evolution profiles of the products with respect to the reaction time. The whole process consisted of two stages: (1) reduction of the catalyst by the bio-compounds; (2) catalytic pyrolysis of the bio-compounds. The occurrence of catalyst reduction was indicated by a CO_2 formation peak and a H_2O formation peak at the initial stage [42]. Following the reduction, catalytic pyrolysis of the bio-compounds occurred. The average gas yield over the pyrolysis stage is summarized in Table 2. Little liquid condensate was formed during the catalytic pyrolysis process and no other carbon-containing gaseous products but CO, CO_2, and CH_4 was detected by gas chromatography (GC). Thus, the yield of solid carbon was calculated by subtracting the carbon fed into the reactor with the carbon in the gaseous products.
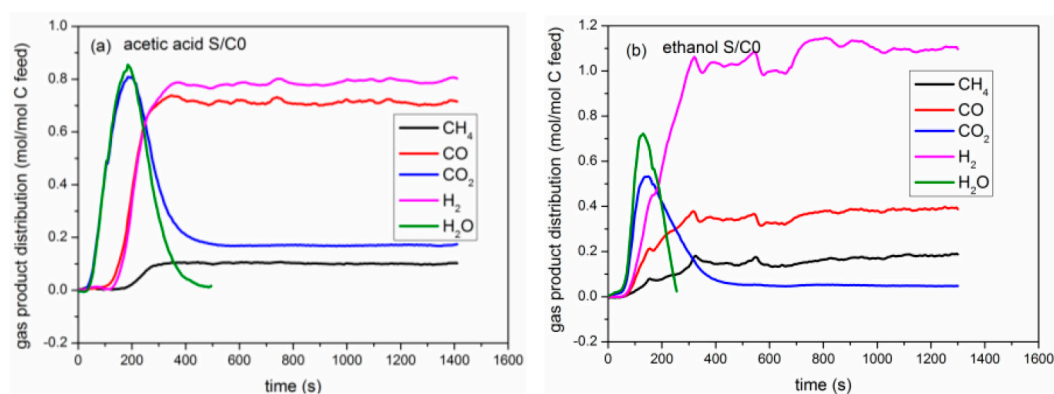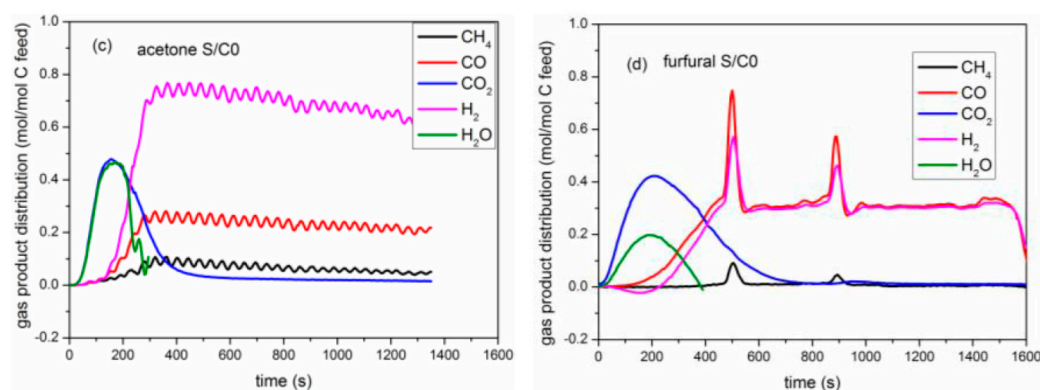
Figure 8. Evolution profiles of products against reaction time during pyrolysis of the bio-compounds at 650 °C and the presence of the NiO/α-Al$_2$O$_3$ catalyst: (**a**) acetic acid, (**b**) ethanol, (**c**) acetone, (**d**) furfural.

Table 2. Yields of H$_2$, CO, CH$_4$, CO$_2$ and solid C (in mol/mol C feed) from catalytic pyrolysis of the bio-compounds.

Bio-Compounds	H$_2$	CO	CO$_2$	CH$_4$	Solid C
acetic acid	0.79	0.71	0.17	0.1	0.02
ethanol	1.08	0.37	0.05	0.16	0.42
acetone	0.68	0.23	0.02	0.06	0.69
furfural	0.31	0.31	0.01	0.01	0.67

During the catalytic pyrolysis stage, H$_2$ and CO were the main products. Small amounts of CH$_4$ and CO$_2$ were also produced. The ratio of the H$_2$ yield to CO yield was related to the H/O ratio in the bio-compound molecules. For acetic acid and furfural (H/O = 2), the H$_2$ yield was close to the CO yield (Figure 8a,d). For ethanol and acetone (H/O = 6), the H$_2$ yield was approximately three times the CO yield (Figure 8b,c). Among the four bio-compounds investigated, the catalytic pyrolysis of ethanol yielded the largest amount of CH$_4$ (0.16 mol CH$_4$ per mol C feed). Acetone and furfural had the strongest tendency to produce carbon deposits during pyrolysis with the yield of solid carbon being more than 60%.

2.4. Effects of S/C

Figure 9 presents the variation of the bio-compound conversion with S/C. In general, high steam content could facilitate both SR and WGS reactions and thus enhance bio-compound conversions. Following this pattern, the conversions of acetic acid and furfural kept increasing as the S/C increased. The conversions of ethanol and acetone also increased until the S/C was up to 3 and 2, respectively. The further addition of steam would not promote their conversions. For glucose, due to the limitation of glucose solubility, the S/C range studied was from 4.5 to 9. As the S/C increased, the glucose conversion increased first and then decreased. For glucose, the maximum conversion was achieved at S/C = 7.5. When the S/C was beyond 7.5, excessive steam might cover active sites of the catalyst and thus impair the adsorption of reactant molecules on the active sites [49].
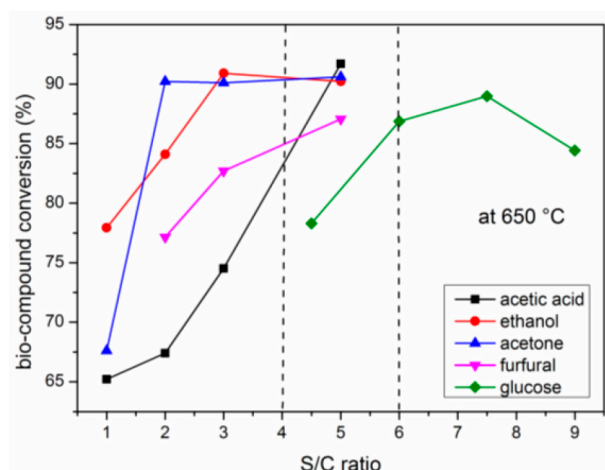
Figure 9. Effects of S/C on bio-compound conversions during SR at 650 °C.

The influence of S/C on the yields of H_2, CO_2, CO, and CH_4 is shown in Figure 10. As Figure 10a shows, the H_2 yield from SR of furfural and acetic acid kept increasing as the S/C increased. The H_2 yield from SR of ethanol and acetone underwent a fast increase first and then a slow increase with the S/C. For glucose, the increase of S/C from 4.5 to 6 caused an increase of the H_2 yield, but a further increase of S/C from 6 to 9 had a negligible effect on the H_2 yield. According to the H_2 yield, the five bio-compounds could be classified into two groups: (1) ethanol and acetone with high H_2 yields; (2) furfural, acetic acid, and glucose with low H_2 yields. Nonetheless, the H_2 yield from SR of glucose at 650 °C and S/C = 6 (1.42 mol/mol C feed) was comparable with the result in ref. [5] (67% of the stoichiometric potential, i.e., 1.34 mol/mol C feed). The small difference between the two H_2 yields might be ascribed to the different $G_{C_1}HSV$ (CH_4-equivalent gas hourly space velocity, defined as the volume of CH_4-equivalent species in the feed at standard temperature and pressure per unit volume of catalyst per hour) values and the different catalysts. With increasing S/C, the CO_2 yield increased while the CO yield decreased as Figure 10b,c show. This was probably because an increase in the S/C promoted the conversion of CO to CO_2 by the WGS reaction. Higher steam content also shifted the equilibrium of the CH_4 SR reaction to the direction of more CH_4 consumption. Thus, the CH_4 yield decreased as Figure 10d shows. When the S/C ratio was above 6, the influence of S/C on the gas yields became less pronounced.
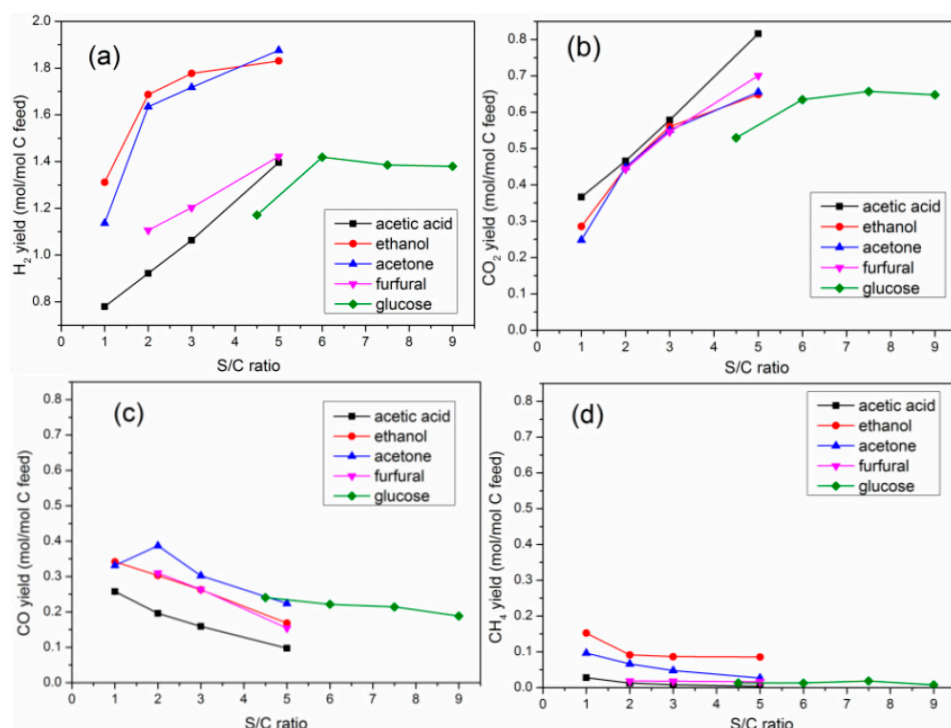
Figure 10. Effects of S/C on gas yields from the SR of bio-compounds with the auto-reduced nickel catalyst at 650 °C: (**a**) H_2, (**b**) CO_2, (**c**) CO, and (**d**) CH_4.

2.5. Micro-Morphology of Carbon Deposits

2.5.1. Acetic Acid, Ethanol, Acetone, and Furfural

Depending on the feedstock and the condition used, the carbon deposited on reforming catalysts may show different morphologies and natures. Previous studies have reported pyrolytic carbon, encapsulating carbon, whisker carbon [39], carbon rickles, and carbon fibers [22]. Figure 11 shows that the SR of acetic acid [50], acetone, ethanol, and furfural all produced carbon filaments, despite slight differences in diameter and density. Carbon filaments from SR of ethanol and furfural (50–100 nm in diameter) were thicker than those from SR of acetic acid and acetone (15–50 nm in diameter). The carbon filaments from SR of acetic acid and furfural (Figure 11a,d) were much denser than those from SR of acetone and ethanol (Figure 11b,c). Similar morphologies of these carbon filaments from SR of acetic acid, acetone, ethanol, and furfural implied similar coking mechanisms for these bio-compounds. The difference in the size and the density of these carbon filaments might further reveal the possible affecting factors of carbon deposition.

The correlation between the morphology of these carbon filaments (size and density) and the amount of carbon deposits (the result of Figure 7 at 650 °C) is shown in Table 3. A general rule was found. The amount of carbon deposits positively correlated with their density. The denser these carbon filaments were, the larger the amount of the carbon filaments was. When the carbon filaments had the same density, the amount of the carbon filaments was related to the diameter of the carbon filaments. The bigger the diameter of the carbon filaments, the larger the amount of the carbon filaments was. These carbon filaments have several negative influences on the SR process. They may impair the activity of catalysts by covering active sites or causing detachment of active metal Ni from the support [39,51,52]. They may also lead to some operation problems by blocking the reactor.
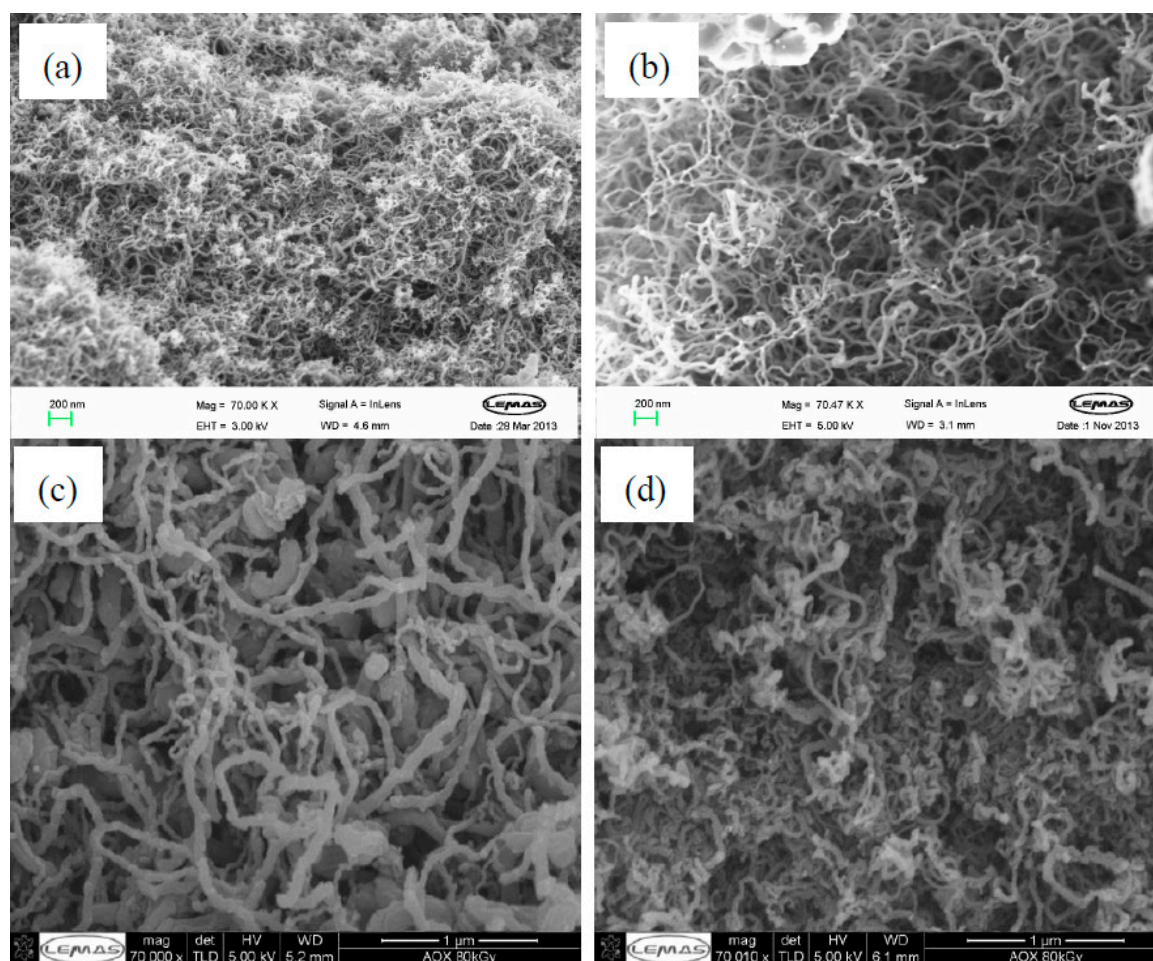
Figure 11. Scanning electron microscope (SEM) images of reacted catalysts from the steam reforming of (**a**) acetic acid, (**b**) acetone, (**c**) ethanol, and (**d**) furfural for a duration of 45 min at conditions of 650 °C and S/C = 3.

Table 3. Correlation between the morphology and the amount of the carbon deposits produced during the SR of furfural, acetic acid, ethanol, and acetone.

Amount of Carbon Deposits in Descending Order	Furfural	Acetic Acid	Ethanol	Acetone
Density of carbon filaments	dense	dense	less dense	less dense
Diameter of carbon filaments	big	small	big	small

2.5.2. Glucose

The carbon deposits formed during SR of glucose exhibited a different morphology, either large smooth flakes on the agglomerated catalyst particles (Figure 12a,b) or a layer of whisker carbon on the non-agglomerated catalyst particles (Figure 12d). The carbon that combined two catalyst particles together was in the form of porous honeycomb (Figure 12c), possibly resulting from gas evolution during the decomposition of "sugar glue". The small granules on the catalyst surface (e.g., sites A, D, and E in Figure 12b,d) were Ni crystallite clusters, indicated by the Energy Dispersive X-ray Spectroscopy (EDX) result in Table 4 and the low angle back-scattered electron (LA-BSE) image (see Supplementary Materials Figure S2). In contrast to SR of the other bio-compounds, the SR of glucose produced carbon deposits with a distinct shape, indicating a different coking mechanism. To corroborate this conjecture, further studies are needed in the future.
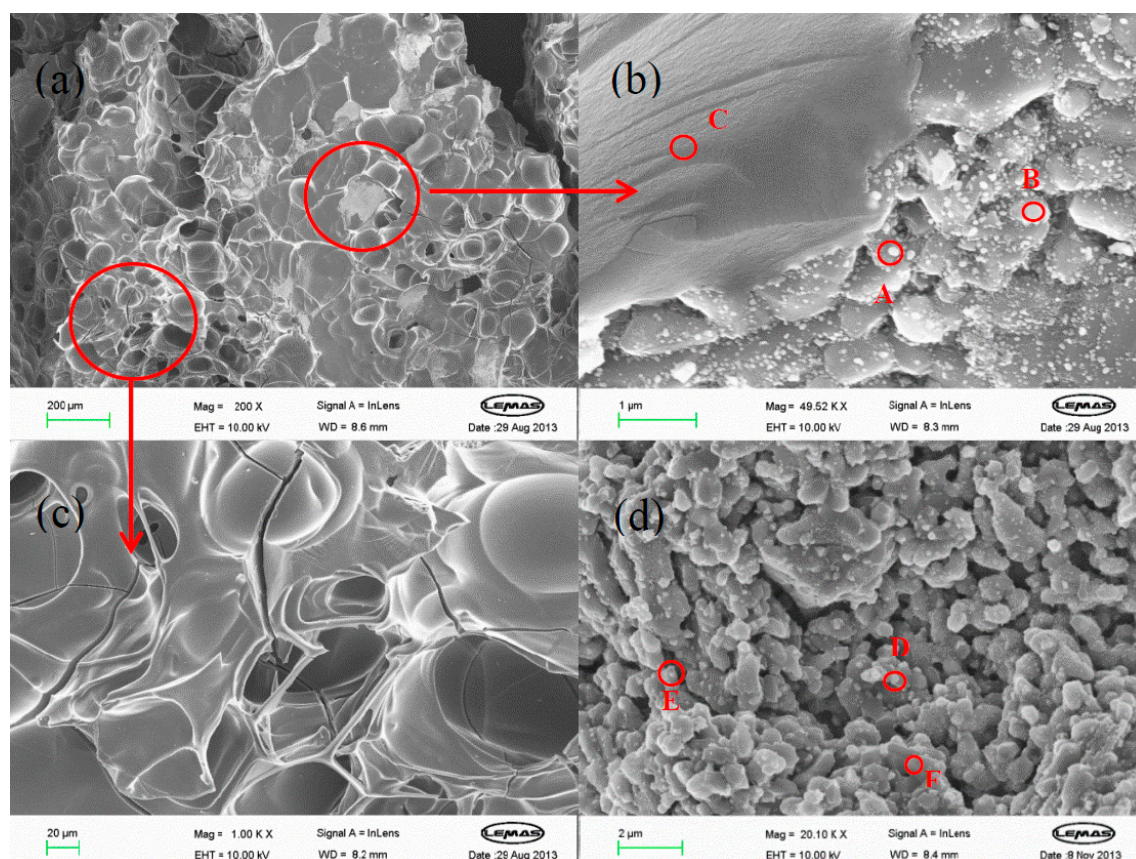
Figure 12. SEM images of (**a–c**) agglomerated catalyst particles and (**d**) non-agglomerated catalyst particles from the steam reforming of glucose at 550 °C, circles A-F are sampling points for Energy Dispersive X-ray Spectroscopy (EDX) analysis.

Table 4. Elemental compositions (in wt %) of different sampling points marked in Figure 12 determined by Energy Dispersive X-ray Spectroscopy (EDX).

Sites	Al	O	Ni	C
A	27	0	42	31
B	51	5	3	41
C	0	6	0	94
D	14	17	59	10
E	28	18	49	5
F	57	41	0	2

3. Materials and Methods

3.1. Materials

The catalyst used in this study was 18 wt % NiO supported on α-Al_2O_3 (NiO/α-Al_2O_3), which was supplied in pellet form by Johnson Matthey Plc (Royston, UK). The NiO/α-Al_2O_3 catalyst pellets were crushed and sieved to particle sizes of 1.0–1.4 mm prior to being used in a packed bed reactor. The bio-compounds studied in this paper include ethanol, acetone, furfural, and glucose, which represent four common chemical families of bio-oil (alcohols, ketones, furans, and sugars). All the bio-compounds were purchased from Sigma-Aldrich and had a purity of >99%.

3.2. Reactor Set-Up and Operation Procedure

A packed bed reactor set-up was employed to perform the auto-reduction and subsequent SR process. Its schematic diagram and the details on the reactor set-up can be found in ref. [42]. For each run of the experiment, 2 g fresh catalyst was placed in the middle of a quartz reactor. The experiment was carried out at atmospheric pressure under a continuous N_2 flow of 200 sccm (MKS mass flow controller, MKS instruments Inc., Andover, MA, USA). When the reactor was heated to a set temperature, liquid feedstock was fed into the reactor by syringe pumps (New Era NE-1000, New Era Pump Systems Inc., Farmingdale, NY, USA). For water-soluble bio-compounds (ethanol, acetone, and glucose), an aqueous solution of bio-compound was made first and then injected into the reactor by one syringe pump. Different S/C ratios were achieved by changing the molar ratio of water to bio-compound in the solution. Furfural and water were fed into the reactor separately by two syringe pumps since furfural was insoluble with water. Different S/C ratios were achieved by setting appropriate flow rates of furfural and water. The flow rate of the carbon equivalent (i.e., the flow rate of the bio-compound multiplied by the number of carbon atoms in the bio-compound molecule) was kept at around 1.174 mmol/min for all the bio-compounds except for glucose. Previous studies [5,10] showed that the SR of glucose had a large tendency for carbon deposition and thus required higher S/C ratios. Therefore, the carbon equivalent input of glucose was 0.6061 mmol/min and the range of S/C ratios investigated for glucose (4.5–9) was larger than that for the other bio-compounds (1–5). The $G_{C1}HSV$ used was 400–800 h^{-1}. The running time of each test was about 3000–4000 s, which enabled an auto-reduction and a steady SR regime of more than 2700 s to be achieved. The present work did not test how long the steady SR performance could last for.

The effluent from the reactor was cooled by a condenser. Condensable products and unreacted water were trapped in a condensate collector. Residual moisture was later removed by silica gel. After that, the molar fraction of CO, H_2, CO_2, and CH_4 in the dry outlet gas was measured by an Advanced Optima gas analyser from ABB (Infra-red absorption for CO, CO_2 and CH_4, thermal conductivity for H_2). Following the gas analyser, a Varian micro gas chromatograph (GC, equipped with MS5 and PPQ columns) was used to detect other possible hydrocarbon gases C_2 (C_2H_4, C_2H_6) and C_3 (C_3H_6, C_3H_8).

As a comparative experiment, the SR of bio-compounds with the H_2-reduced catalyst was also performed in this reactor set-up. When the reactor was heated to 650 °C, a N_2 gas flow with 5% H_2 at a rate of 300 sccm was switched on and continuously flowed through the fresh catalyst bed until the H_2 concentration in the outlet gas returned to 5%. This process approximately took 17 min. After this, the gas flow of 5% H_2/N_2 was maintained for another 30 min to ensure the reduction was complete. Then the 5% H_2/N_2 gas flow was switched off. Following a N_2 purge, the SR experiments of bio-compounds were started.

3.3. Elemental Balance and Definition of Process Outputs

The molar flow rate of total dry outlet gas ($n_{out,dry}$) was estimated based on the nitrogen balance (Equation (1)). The molar flow rate of N_2 (n_{N_2}) was maintained at 1.386×10^{-4} mol/s, equivalent to a volume flow rate of 200 sccm during the experimental process. The conversion of the bio-compound (X_{bio}) to gases was calculated based on the carbon balance, dividing the total molar flow of carbon in the gaseous products by the molar flow of carbon in the feed, as described in Equation (2). The H_2O conversion (X_{H_2O}) was calculated on the basis of hydrogen balance (Equation (3)). The yield of gas *i* was defined as the moles of gas *i* produced per mole of carbon feed (Equation (4)). The yield of carbon deposits during SR of bio-compounds was calculated using Equation (5). The gas concentration of species *i* was defined as the molar fraction of *i* in dry outlet gas divided by the sum of molar fractions of all the product gases (excluding N_2). H_2 yield efficiency was defined as the percentage of experimental H_2 yield with respect to the equilibrium values.

$$n_{\text{out,dry}} = \frac{n_{N_2}}{1 - y_{CH_4} - y_{CO} - y_{CO_2} - y_{H_2} - y_{C_2} - y_{C_3}} \tag{1}$$

$$X_{\text{bio}} = \frac{n_{\text{out,dry}} \times (y_{\text{CO}} + y_{\text{CO}_2} + y_{\text{CH}_4} + 2y_{\text{C}_2} + 3y_{\text{C}_3})}{n \times n_{\text{bio,in}}} \qquad (2)$$

$$X_{\text{H}_2\text{O}} = \frac{n_{\text{out,dry}} \times (4y_{\text{CH}_4} + 2y_{\text{H}_2} + 4y_{\text{C}_2\text{H}_4} + 6y_{\text{C}_2\text{H}_6} + 6y_{\text{C}_3\text{H}_6} + 8y_{\text{C}_3\text{H}_8}) - m \times n_{\text{bio,in}} \times X_{\text{bio}}}{2\, n_{\text{H}_2\text{O,in}}} \qquad (3)$$

$$\text{gas yield (mol/mol carbon feed)} = \frac{n_{\text{out,dry}} \times y_i}{n \times n_{\text{bio,in}}} \qquad (4)$$

$$\text{C yield} = \frac{\text{catalyst mass} \times \text{carbon content (wt \%)}/12}{\text{carbon feed} \left(\text{in } \frac{\text{mol}}{\text{s}}\right) \times \text{reaction duration}} \qquad (5)$$

Nomenclature:

n_i: flow rate of specie *i* in mol/s

y_i: molar fraction of specie *i* in the dry outlet gas

X_i: conversion fraction of specie *i*

$y_{\text{C}_2} = y_{\text{C}_2\text{H}_4} + y_{\text{C}_2\text{H}_6}$

$y_{\text{C}_3} = y_{\text{C}_3\text{H}_6} + y_{\text{C}_3\text{H}_8}$

$C_n H_m O_k$: a generic formula of the bio-compounds

The subscript "dry", "in", and "out" refer to conditions following water removal, and at reactor inlet and outlet, respectively.

3.4. Material Characterisation

The carbon content on the reacted catalyst was measured by a CHN elemental analyser (Flash EA2000 by CE Instruments Ltd., Wigan, UK). A field-emission scanning electron microscope (SEM, LEO 1530, Oberkochen, Germany) coupled with an energy dispersive X-ray spectrometer (EDX, Oxford Instruments plc, Abingdon, UK) was employed to show the morphology and element distribution of the reacted catalysts. The EDX analysis was made on points of interest rather than zones. In order to clearly show the location of these sampling points, circles were used to mark these points in corresponding SEM images.

3.5. Chemical Equilibrium Calculation

The calculation of equilibrium composition was based on the Gibbs free energy minimization and implemented using the CEA (Chemical Equilibrium with Application) program from National Aeronautics and Space Administration (NASA). The temperature range covered in the calculation was 550–750 °C and the pressure was fixed at 1 atm. In order to calculate the total moles of equilibrium products per mole of initial reactant mixture, a small amount of argon (0.01 mol) was added to the initial reactant mix as an interior label.

4. Conclusions

Steam reforming (SR) of four common bio-compounds (ethanol, acetone, furfural, and glucose) with the auto-reduced NiO/α-Al_2O_3 catalyst was investigated. The SR performance was close to that using H_2-reduced catalyst over the duration of 45–60 min, and was affected by the temperature and S/C ratio. In general, an increase in temperature or S/C could enhance conversions of the bio-compounds and H_2 yields. The dependence of bio-compound conversions and H_2 yields on temperature or S/C was specific to the type of bio-compounds. In addition, the amount and the morphology of the carbon deposits also relied on the bio-compound that was used.

For each bio-compound, the bottleneck of its SR reaction was identified. The main problem for SR of ethanol was a high CH_4 yield that was probably caused by ethanol decomposition. According to previous studies, this problem was common to neutral alcohols and could be solved by acidification of the reforming feedstock. For SR of acetone, severe carbon deposition occurred when the temperature was below 650 °C. Thus, it is essential to ensure the operation temperature is ≥650 °C. The SR of furfural was restricted by the thermal stability of furfural molecules and also severe carbon deposition. Increasing the temperature above 600 °C could overcome the problem of

thermal stability but was less effective for reducing carbon deposits. Therefore, designing an adequate catalyst or using a higher S/C may be desirable for SR of furfural. The main barrier for SR of glucose was the severe agglomeration of catalyst particles due to glucose coking. In order to avoid this agglomeration, the temperature for SR of glucose should be above 650 °C.

Supplementary Materials: The following are available online at www.mdpi.com/2073-4344/7/4/114/s1, Figure S1: Dry gas composition from steam reforming of bio-compounds with the auto-reduced catalyst. (a) acetic acid; (b) ethanol; (**c**) acetone; (d) furfural; (e) glucose, Figure S2: SEM image (LA-BSE signal) of the Ni catalyst (a) 20 k magnification, (b) 70 k magnification.

Author Contributions: Feng Cheng and Valerie Dupont conceived and designed the experiments; Feng Cheng performed the experiments, analyzed the data, and wrote the paper; Valerie Dupont gave comments and edits on the paper.

Conflicts of Interest: The authors declare no conflict of interest. The founding sponsors had no role in the design of the study; in the collection, analyses, or interpretation of data; in the writing of the manuscript, and in the decision to publish the results. This manuscript has not been published or presented elsewhere in part or entirety and it is not under consideration by another journal. All the authors have approved the manuscript and agreed to its submission to your esteemed journal.

References

1. Tanksale, A.; Beltramini, J.N.; Lu, G.M. A review of catalytic hydrogen production processes from biomass. *Renew. Sustain. Energy Rev.* **2010**, *14*, 166–182.
2. Cortright, R.D.; Davda, R.R.; Dumesic, J.A. Hydrogen from catalytic reforming of biomass-derived hydrocarbons in liquid water. *Nature* **2002**, *418*, 964–967.
3. Garcia-Perez, M.; Chaala, A.; Pakdel, H.; Kretschmer, D.; Roy, C. Characterization of bio-oils in chemical families. *Biomass Bioenergy* **2007**, *31*, 222–242.
4. Wang, D.; Czernik, S.; Montane, D.; Mann, M.; Chornet, E. Biomass to hydrogen via fast pyrolysis and catalytic steam reforming of the pyrolysis oil or its fractions. *Ind. Eng. Chem. Res.* **1997**, *36*, 1507–1518.
5. Marquevich, M.; Czernik, S.; Chornet, E.; Montané, D. Hydrogen from biomass: Steam reforming of model compounds of fast-pyrolysis oil. *Energy Fuels* **1999**, *13*, 1160–1166.
6. Fatsikostas, A.N.; Verykios, X.E. Reaction network of steam reforming of ethanol over Ni-based catalysts. *J. Catal.* **2004**, *225*, 439–452.
7. Wang, D.; Montane, D.; Chornet, E. Catalytic steam reforming of biomass-derived oxygenates: Acetic acid and hydroxyacetaldehyde. *Appl. Catal. A* **1996**, *143*, 245–270.
8. Basagiannis, A.C.; Verykios, X.E. Reforming reactions of acetic acid on nickel catalysts over a wide temperature range. *Appl. Catal. A* **2006**, *308*, 182–193.
9. Ramos, M.C.; Navascués, A.I.; García, L.; Bilbao, R. Hydrogen production by catalytic steam reforming of acetol, a model compound of bio-oil. *Ind. Eng. Chem. Res.* **2007**, *46*, 2399–2406.
10. Hu, X.; Lu, G. Investigation of the steam reforming of a series of model compounds derived from bio-oil for hydrogen production. *Appl. Catal. B* **2009**, *88*, 376–385.
11. Graschinsky, C.; Giunta, P.; Amadeo, N.; Laborde, M. Thermodynamic analysis of hydrogen production by autothermal reforming of ethanol. *Int. J. Hydrogen Energy* **2012**, *37*, 10118–10124.
12. Subramani, V.; Song, C. Advances in catalysis and processes for hydrogen production from ethanol reforming. *Catalysis* **2007**, *20*, 65–106.
13. Vagia, E.C.; Lemonidou, A.A. Thermodynamic analysis of hydrogen production via steam reforming of selected components of aqueous bio-oil fraction. *Int. J. Hydrogen Energy* **2007**, *32*, 212–223.
14. Sun, S.; Yan, W.; Sun, P.; Chen, J. Thermodynamic analysis of ethanol reforming for hydrogen production. *Energy* **2012**, *44*, 911–924.
15. Konsolakis, M.; Ioakimidis, Z.; Kraia, T.; Marnellos, G. Hydrogen production by ethanol steam reforming (ESR) over CeO_2 supported transition metal (Fe, Co, Ni, Cu) catalysts: Insight into the structure-activity relationship. *Catalysts* **2016**, *6*, 39.

16. Cifuentes, B.; Figueredo, M.; Cobo, M. Response surface methodology and aspen plus integration for the simulation of the catalytic steam reforming of ethanol. *Catalysts* **2017**, *7*, 15.

17. Cifuentes, B.; Valero, M.; Conesa, J.; Cobo, M. Hydrogen production by steam reforming of ethanol on Rh-Pt catalysts: Influence of CeO_2, ZrO_2, and La_2O_3 as supports. *Catalysts* **2015**, *5*, 1872.

18. Vaidya, P.D.; Rodrigues, A.E. Insight into steam reforming of ethanol to produce hydrogen for fuel cells. *Chem. Eng. J.* **2006**, *117*, 39–49.

19. Contreras, J.L.; Salmones, J.; Colin-Luna, J.A.; Nuno, L.; Quintana, B.; Cordova, I.; Zeifert, B.; Tapia, C.; Fuentes, G.A. Catalysts for H_2 production using the ethanol steam reforming (a review). *Int. J. Hydrogen Energy* **2014**, *39*, 18835–18853.

20. Wang, Y.; Chen, M.; Liang, T.; Yang, Z.; Yang, J.; Liu, S. Hydrogen generation from catalytic steam reforming of acetic acid by Ni/attapulgite catalysts. *Catalysts* **2016**, *6*, 172.

21. Adhikari, S.; Fernando, S.; Gwaltney, S.R.; Filip To, S.; Mark Bricka, R.; Steele, P.H.; Haryanto, A. A thermodynamic analysis of hydrogen production by steam reforming of glycerol. *Int. J. Hydrogen Energy* **2007**, *32*, 2875–2880.

22. Wu, C.; Liu, R. Carbon deposition behavior in steam reforming of bio-oil model compound for hydrogen production. *Int. J. Hydrogen Energy* **2010**, *35*, 7386–7398.

23. Khzouz, M.; Wood, J.; Pollet, B.; Bujalski, W. Characterization and activity test of commercial Ni/Al_2O_3, $Cu/ZnO/Al_2O_3$ and prepared Ni–Cu/Al_2O_3 catalysts for hydrogen production from methane and methanol fuels. *Int. J. Hydrogen Energy* **2013**, *38*, 1664–1675.

24. Yang, X.; Wang, Y.; Wang, Y. Significantly improved catalytic performance of Ni-based MgO catalyst in steam reforming of phenol by inducing mesostructure. *Catalysts* **2015**, *5*, 1721.

25. Hu, X.; Lu, G.X. Investigation of the effects of molecular structure on oxygenated hydrocarbon steam re-forming. *Energy Fuels* **2009**, *23*, 926–933.

26. Remon, J.; Broust, F.; Volle, G.; Garcia, L.; Arauzo, J. Hydrogen production from pine and poplar bio-oils by catalytic steam reforming. Influence of the bio-oil composition on the process. *Int. J. Hydrogen Energy* **2015**, *40*, 5593–5608.

27. Dupont, V.; Ross, A.; Knight, E.; Hanley, I.; Twigg, M. Production of hydrogen by unmixed steam reforming of methane. *Chem. Eng. Sci.* **2008**, *63*, 2966–2979.

28. Pimenidou, P.; Rickett, G.; Dupont, V.; Twigg, M. Chemical looping reforming of waste cooking oil in packed bed reactor. *Bioresour. Technol.* **2010**, *101*, 6389–6397.

29. Giannakeas, N.; Lea-Langton, A.; Dupont, V.; Twigg, M.V. Hydrogen from scrap tyre oil via steam reforming and chemical looping in a packed bed reactor. *Appl. Catal. B* **2012**, *126*, 249–257.

30. Zafar, Q.; Mattisson, T.; Gevert, B. Integrated hydrogen and power production with CO_2 capture using chemical-looping reforming redox reactivity of particles of CuO, Mn_2O_3, NiO, and Fe_2O_3 using SiO_2 as a support. *Ind. Eng. Chem. Res.* **2005**, *44*, 3485–3496.

31. Lyon, R.K.; Cole, J.A. Unmixed combustion: An alternative to fire. *Combust. Flame* **2000**, *121*, 249–261.

32. Mendiara, T.; Johansen, J.M.; Utrilla, R.; Geraldo, P.; Jensen, A.D.; Glarborg, P. Evaluation of different oxygen carriers for biomass tar reforming (I): Carbon deposition in experiments with toluene. *Fuel* **2011**, *90*, 1049–1060.

33. Adanez, J.; Abad, A.; Garcia-Labiano, F.; Gayan, P.; de Diego, L.F. Progress in chemical-looping combustion and reforming technologies. *Prog. Energy Combust. Sci.* **2012**, *38*, 215–282.

34. Dou, B.; Song, Y.; Wang, C.; Chen, H.; Yang, M.; Xu, Y. Hydrogen production by enhanced-sorption chemical looping steam reforming of glycerol in moving-bed reactors. *Appl. Energy* **2014**, *130*, 342–349.

35. Pimenidou, P.; Rickett, G.; Dupont, V.; Twigg, M.V. High purity H_2 by sorption-enhanced chemical looping reforming of waste cooking oil in a packed bed reactor. *Bioresour. Technol.* **2010**, *101*, 9279–9286.

36. Cheng, F.; Dupont, V.; Twigg, M.V. Direct reduction of nickel catalyst with model bio-compounds. *Appl. Catal. B* **2017**, *200*, 121–132.

37. Tribalis, A.; Panagiotou, G.; Bourikas, K.; Sygellou, L.; Kennou, S.; Ladas, S.; Lycourghiotis, A.; Kordulis, C. Ni catalysts supported on modified alumina for diesel steam reforming. *Catalysts* **2016**, *6*, 11.

38. Goodman, D.R. *Catalyst Handbook*, 2nd ed.; Twigg, M.V., Ed.; Wolfe Publishing Ltd.: London, UK, 1996; pp. 161–174.

39. Sehested, J. Four challenges for nickel steam-reforming catalysts. *Catal. Today* **2006**, *111*, 103–110.

40. Lea-Langton, A.; Zin, R.M.; Dupont, V.; Twigg, M.V. Biomass pyrolysis oils for hydrogen production using chemical looping reforming. *Int. J. Hydrogen Energy* **2012**, *37*, 2037–2043.

41. Dupont, V.; Ross, A.B.; Hanley, I.; Twigg, M.V. Unmixed steam reforming of methane and sunflower oil: A single-reactor process for H_2-rich gas. *Int. J. Hydrogen Energy* **2007**, *32*, 67–79.

42. Feng, C.; Dupont, V. Nickel catalyst auto-reduction during steam reforming of bio-oil model compound acetic acid. *Int. J. Hydrogen Energy* **2013**, *38*, 15160–15172.

43. Cheng, F. Bio-Compounds as Reducing Agents of Reforming Catalyst and Their Subsequent Steam Reforming Performance. Ph.D. Thesis, University of Leeds, Leeds, UK, 2014.

44. Kato, K.; Takahashi, N. Pyrolysis of cellulose part II. Thermogravimetric analyses and determination of carbonyl and carboxyl groups in pyrocellulose. *Agric. Biol. Chem.* **1967**, *31*, 519–524.

45. Wu, C.; Liu, R. Hydrogen production from steam reforming of *m*-cresol, a model compound derived from bio-oil: Green process evaluation based on liquid condensate recycling. *Energy Fuels* **2010**, *24*, 5139–5147.

46. Fagerson, I.S. Thermal degradation of carbohydrates; a review. *J. Agric. Food Chem.* **1969**, *17*, 747–750.

47. Sugisawa, H.; Edo, H. The thermal degradation of sugars I. Thermal polymerization of glucose. *J. Food Sci.* **1966**, *31*, 561–565.

48. Örsi, F. Kinetic studies on the thermal decomposition of glucose and fructose. *J. Therm. Anal.* **1973**, *5*, 329–335.

49. Gardner, R.A. The kinetics of silica reduction in hydrogen. *J. Solid State Chem.* **1974**, *9*, 336–344.

50. Vagia, E.C.; Lemonidou, A.A. Investigations on the properties of ceria–zirconia-supported Ni and Rh catalysts and their performance in acetic acid steam reforming. *J. Catal.* **2010**, *269*, 388–396.

51. Rossetti, I.; Lasso, J.; Nichele, V.; Signoretto, M.; Finocchio, E.; Ramis, G.; Di Michele, A. Silica and zirconia supported catalysts for the low-temperature ethanol steam reforming. *Appl. Catal. B* **2014**, *150–151*, 257–267.

52. Rossetti, I.; Gallo, A.; Dal Santo, V.; Bianchi, C.L.; Nichele, V.; Signoretto, M.; Finocchio, E.; Ramis, G.; Di Michele, A. Nickel catalysts supported over TiO_2, SiO_2 and ZrO_2 for the steam reforming of glycerol. *ChemCatChem* **2013**, *5*, 294–306.